Insights into the magnetic properties and hydrogen interaction characteristics of the Au_9M (M = Y and Mo) systems

Lan Ngo Thi[1], Dang Nguyen Van[1*] Hien Trinh Ngoc[3], Thanh Huyen Nguyen Thi[1], Ha Le Tien[1], Mai Nguyen Thi[2], Tung Nguyen Thanh[2]

[1]*TNU-University of Sciences, Phan Dinh Phung Ward, Thai Nguyen Province, Vietnam*

[2]*Institute of Materials Science, Vietnam Academy of Science and Technology, 18 Hoang Quoc Viet Street, Nghia Do Ward, Hanoi, Vietnam*

[3]*TNU-University of Information and Communication Technology, Phan Dinh Phung Ward, Thai Nguyen Province, Vietnam*

Received 10 February 2026; revised 11 February 2026; accepted 28 March 2026

Abstract:

The *s-d* hybridisation in bimetallic nanocluster systems constitutes a fascinating topic that has recently garnered significant interest from researchers. In this work, we compared the effects of electronic configurations on the magnetic properties and hydrogen interaction capabilities of the Au_9Y and Au_9Mo clusters using density functional theory calculations. The singlet Au_9Y is nonmagnetic, whereas the quartet Au_9Mo exhibits a magnetic moment of 3 μB, which is consistent with their electronic configurations $1S^21P^61D^4$ and $1S^21P^61D^64d_{Mo}^3$, respectively. Spin density analysis reveals that the origin of the magnetic moment is primarily due to the localisation of electrons within 4*d*-M orbitals. We also report the possible infrared vibrational spectra of $Au_9M@H_2$ (M = Mo and Y), which have not been documented in the literature to date. We anticipate that our results will enhance the theoretical understanding of $Au_9M@H_2$ clusters and aid experimental efforts to elucidate the structure of Au_9M species.

Keywords: **density functional theory, gold clusters, infrared spectrum, magnetic moment.**

Classification number: **2.2**

[*]*Corresponding author: Email: dangnv@tnus.edu.vn*

1. Introduction

Bimetallic gold clusters have recently attracted significant attention from researchers due to their unique physical and chemical properties. Gold in its neutral state is known to be chemically inert. However, at the nanoscale, gold shows unique magnetic properties [1-3] and exhibits high catalytic activity [4, 5]. This makes it significant in various processes, including CO oxidation [6], NO reduction [7], and hydrogen storage [8]. Many studies have emphasised that the *s-d* interactions in gold nanoclusters containing transition metal atoms provide an intriguing picture of the magnetic properties and catalytic capabilities of these clusters. For example, variations in the magnetic spin moment of gold clusters with transition metals have been observed to correlate with the strong hybridisation between the s-Au and d-M orbitals of the dopant atoms [9, 10]. The magnetic moment of noble metal clusters (Au_n, Ag_n, and Cu_n) is significantly influenced by the hybridisation between the valence electrons of the vanadium atoms and the host cluster [11]. The position of the Fe dopant atom plays a crucial role in determining the electronic and magnetic structure of the $Au_{18}Fe$ and $Au_{19}Fe$ clusters, as explored by Ehlert, et al. (2019) [12]. Subsequently, the research group of N.T. Lan and N.T. Mai indicated that the strong hybridisation between the s orbital of the gold (Au) host and the 3d orbitals of the transition metal atoms results in the coexistence of delocalised and localised electrons in nanoclusters [9, 13, 14]. Notably, both Au_9Cr^{2+} and $Au_{19}Cr$ clusters exhibit closed electronic shells with 8 and 18 electrons, respectively, corresponding to the electronic configurations of $1S^21P^42S^2$ and $1S^21P^61D^{10}$. The remaining five electrons do not engage in hybridisation to form the electronic structure and are localised in the 3*d*-Cr orbital, suggesting that these species may function as potential superatoms with an associated magnetic moment of 5 μB. Furthermore, the research group also demonstrated that the electronic structure plays a crucial role in the interaction with hydrogen, with Au_9Ti^{2+} acting as a potential superatom in the

hydrogen adsorption and storage process, facilitating hydride formation at room temperature [15].

The impact of electrical anharmonicity on the infrared band profile of hydrogen bonds has been investigated by N. Rekik, et al. (2010, 2017) [16, 17]. The IR spectra of weak hydrogen-bond complexes have been elucidated using linear response theory and quantum theory of the high-stretching-mode spectral density [18]. Subsequently, the influence of vibrational exciton interactions in onxindole crystals on hydrogen bonds, as well as the dissimilarity of the IR spectral density of dicarboxylic acid crystals, has been investigated [19, 20]. Recently, the interaction capabilities of gold clusters doped with 4d transition metal atoms with hydrogen, aimed at applications in energy storage materials, have been initially explored by N.V. Dang, et al. (2025a, 2025b) [21, 22]. However, the research has not yet clarified how delocalised and localised electronic structures form, nor the roles of these free and localised electrons in their interaction with hydrogen in these material systems. It is important to emphasise that the Mo atom has more unpaired electrons than the Y atom, specifically possessing an outer electron configuration of Mo: $4d^5 5s^1$ compared to Y: $4d^1 5s^2$. This characteristic is expected to create distinct patterns of participation and electron-exchange processes within nanocluster systems. Motivated by the quest to understand the effect of electronic structure on hydrogen-storage nanostructured materials, this study aims to theoretically compare the significant roles of Y and Mo dopants in magnetism and H_2 adsorption and dissociation within the Au_9M (M = Y and Mo) system. These findings underscore the importance of electronic structure formation in magnetism, adsorption, and hydrogen storage materials, promising advances in clean energy technology applications.

2. Computational method

In this work, we investigated the ground-state geometries and electronic structures of Au_9M, their molecular (Au_9M-H_2) and dissociative (Au_9M-2H) adsorbed species (M = Y and Mo). These calculations were performed using the density functional theory (DFT) approach as implemented in the Gaussian 09 package [23, 24]. The search structures were initially optimised using the TPSSTPSS functional combination with the cc-pVDZ-pp basis set for Au and M atoms, while the LanL2DZ basis set was employed for H atoms. Then, isomers with relative energies less than 2.0 eV were selected for recalculation of single-point energies using the same level of theory but with the larger cc-pVTZ-pp for Au and M atoms. The feasibility of the TPSSTPSS functional was confirmed by previous publications [21, 22, 25]. The convergence criteria for geometrical optimisation are set at 2.0 x 10^{-5} Hartree/Å, 4.0 x 10^{-3} Hartree, and 5.0 x 10^{-3} Å for the energy change, the gradient, and the displacements, respectively. The electronic configurations of the ground-state Au_9M and the hydrogen interaction characteristics of $Au_9M@H_2$ (M = Y and Mo) were explored using spin density and infrared (IR) vibrational spectra. The total/local magnetic moments (TMMs/LMMs) were defined as the difference between the numbers of spin-up and spin-down electrons occupying the molecular/atomic orbitals of the cluster/atom.

3. Results and discussion

3.1. The optimal geometric and spin multiplicities

To investigate the influence of doping transition metal atoms (Y and Mo) on the properties of pure gold clusters, we performed a search for stable geometric structures and electronic configurations of the clusters. First, the lowest-lying structure and spin state of the pure gold cluster Au_{10} were identified. Subsequently, Y and Mo atoms were sequentially substituted for an Au atom at all possible positions within the stable geometric structure of Au_{10}. These configurations served as the input structures for subsequent calculations. The stable geometric

structures and spin states of the Au_9Y and Au_9Mo clusters are depicted in Fig. 1. In the following sections, the isomers are labelled in the form 9.M.X/N^m, where M = Y and Mo, and X = A, B, and C refer to the different isomers with increasing relative energy N. The subscript m denotes spin multiplicity.

Au_9Y: The computed lowest-lying energy structure of singlet 9.Y.A, in which Y is encapsulated by a distorted seven-sided surface, is considered the stable geometric structure. The next isomers, singlet 9.Y.B and singlet 9.Y.C, are highly unstable, exhibiting relative energies of 0.15 eV and 0.41 eV, respectively, compared with the most stable 9.Y.A.

Au_9Mo: Our computed global minimum-energy isomer, quartet 9.Mo.A adopts a cross-section of an icosahedral cage. In this structure, the Mo atom preferentially substitutes for the Au atom at the central position of the symmetric hexagon. Although the next isomer, doublet 9.Mo.B experiences a distortion of the cross-section of the icosahedral cage, the Mo atom is preferentially retained in the same position as in 9.Mo.A. The difference in energy between 9.Mo.B and the corresponding ground-state structure is 0.06 eV. In contrast, the relative energy of the less stable doublet 9.Mo.C is 0.1 eV higher than that of the ground state.

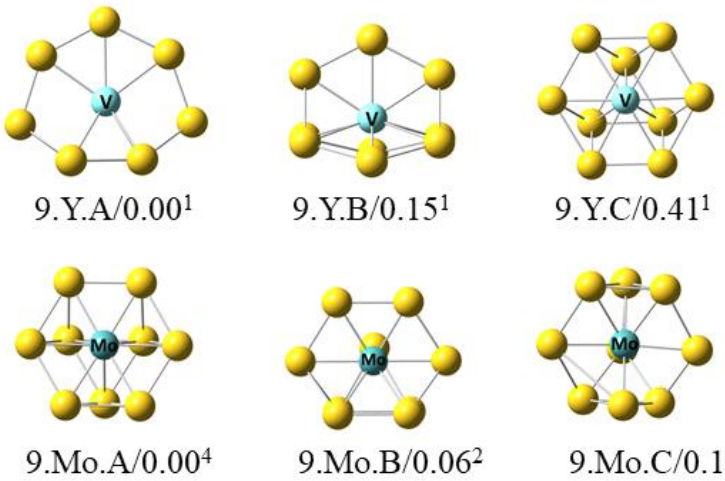

Fig. 1. Optimised structures, spin multiplicities, and relative energies (in eV) of the lowest-lying isomers of Au_9M (M = Y and Mo). The yellow, cyan, and dark cyan spheres represent are Au, Y, and Mo atoms, respectively.

3.2. Electronic configuration and magnetic properties

The incorporation of transition metal atoms Y and Mo into the Au_9 cluster yields entirely distinct results. The magnetic properties of the Au_9Y cluster are completely quenched, while the magnetic moment of the Au_9Mo cluster is 3 μ_B. The primary goal of this work is to clarify the influence of *s-d* interactions on the magnetic differences between the two cluster systems, thereby facilitating the systematisation of predictions regarding electronic properties in analogous quantum systems. By retaining the structure of the Au_9 cluster and doping it with transition metal atoms featuring different valence electron configurations (Y: $4d^15s^2$ and Mo: $5s^14d^5$), two interesting contrasting pictures are revealed. First, the geometric structure of the Au_9Y cluster is a distorted seven-sided shape, while the Au_9Mo cluster favours the form of a cross-section of an icosahedral cage. This results in the formation of distinct electronic configurations. Specifically, assuming that each gold atom delocalises one $6s^1$ electron, Au_9Y and Au_9Mo clusters provide a total of 12 and 15 electrons, respectively. However, the contributions of the valence electrons from Y and Mo to the formation of the electronic shell structure of these dopant species differ. For the case of the Au_9Y cluster, all $4d^15s^2$ valence electrons of Y delocalise and join with the s valence electrons of the Au host. The total number of valence electrons in the Au_9Y cluster is 12 (9 from Au atoms and 3 from Y dopant), resulting in electronic configurations of $1S^21P^61D^4$. In other words, the strong hybridisation between $6s^1$-Au and 4*d*-Y orbitals results in the complete quenching of the magnetic moment in the Au_9Y cluster. In the opposite picture for Au_9Mo, only three valence electrons from Mo (one $5s^1$ and two $4d^5$) take part in the hybridisation involved in the formation of the electronic shell structure. The remaining three electrons are localised on 4*d*-Mo atomic orbitals, giving rise to the magnetic moment of the cluster, which is 3 μB. This suggests that the magnetism of the cluster is primarily attributed to the localized electrons in the 4d-orbitals of the dopant atom. This behaviour aligns with previous studies on the magnetism of clusters included by

the delocalisation of 3d-transition metal dopants in gold clusters [26]. The strong hybridisation of s-d interaction in Au_5Sc^+ results in the complete quenching of magnetism while the Au_5Cr^+ cluster exhibits strong magnetism with a high magnetic moment of 4 μB [27]. The same observation can be found in the cations/neutral/cations of the system comprising transition metals and the Ag_n, Cu_n doped with 3d transition metal atoms (Sc-Ni) [9, 13, 28-32].

In the following, we further verify the origin of the cluster magnetic behaviour by mapping the spin-up and spin-down densities in Au_9Y and Au_9Mo clusters. The results are shown in Fig. 2. It is worth mentioning that the total spin of the Au_9Mo cluster is mainly located at the position of the Mo dopant atom. This result agrees with our discussion above that the total magnetic moment of Au_9Mo cluster essentially comes from the localised 4d dopant electrons. Consequently, the exact electronic configuration can be assigned as $1S^21P^61D^44d_{Mo}^3$. An opposite picture is seen for the Au_9Y cluster; the local magnetic moment of the Y dopant atom disappears, and the spin-up and spin-down clouds entirely overlap. This can be explained by the fact that all of the valence electrons in Y delocalise to form the electronic shells of the cluster. The differences in the predicted electronic configurations provide a novel perspective on the interaction capabilities with hydrogen. This issue will be further discussed in the following section.

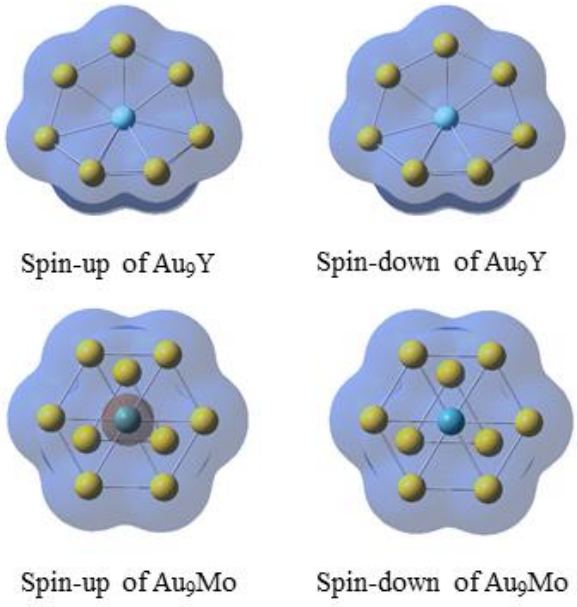

Fig. 2. Spin density of the ground-state Au_9Y and Au_9Mo clusters.

3.3. Hydrogen adsorption characterisation

To date, numerous studies employing quantum computational approaches have indicated that the shape of the infrared spectral density of hydrogen bonds significantly depends on the structure and composition of the material system [33-38]. However, several studies have shown that the localised electrons of the transition metal dopant atom contribute not only to the magnetic moment of clusters but also significantly influence interactions with hydrogen [15, 21, 39-41]. The calculated adsorption energies indicate that the negative adsorption energy for Au_9Y-2H (-0.11 eV) suggests that dissociative adsorption in this species is endothermic and unlikely to occur spontaneously. Conversely, for the Au_9Mo cluster, the dissociative adsorption energy (Au_9Mo-2H: 0.66 eV) is higher than the molecular adsorption energy (Au_9Mo-H_2: 0.65 eV). It can be stated that the two states are energetically nearly degenerate, with the observed difference being negligible (0.01 eV). Furthermore, the reaction dynamics calculations indicate that the Au_9Mo cluster is a promising candidate for hydrogen adsorption, with a very low activation barrier for the dissociative adsorption process and the reverse process [22].

Studies on the characteristics and binding mechanisms of hydrogen-bonded dimers in various systems, utilising comprehensive quantum computational approaches, have been theoretically investigated by N. Rekik, et al. (2001, 2012) [42-46]. In the following sections, we investigate the vibrational characteristics of the clusters by calculating the infrared (IR) vibrational spectra. The results are displayed in Fig. 3. Upon initial examination, the observed adsorption peaks can be clearly categorised into opposing patterns. For the molecularly adsorbed Au_9Y-H_2 cluster, peaks are observed in the extended frequency range of 0-4500 cm^{-1}, while dissociative adsorption of the Au_9Mo-2H cluster is primarily observed in the lower frequency range of 0-2000 cm^{-1}.

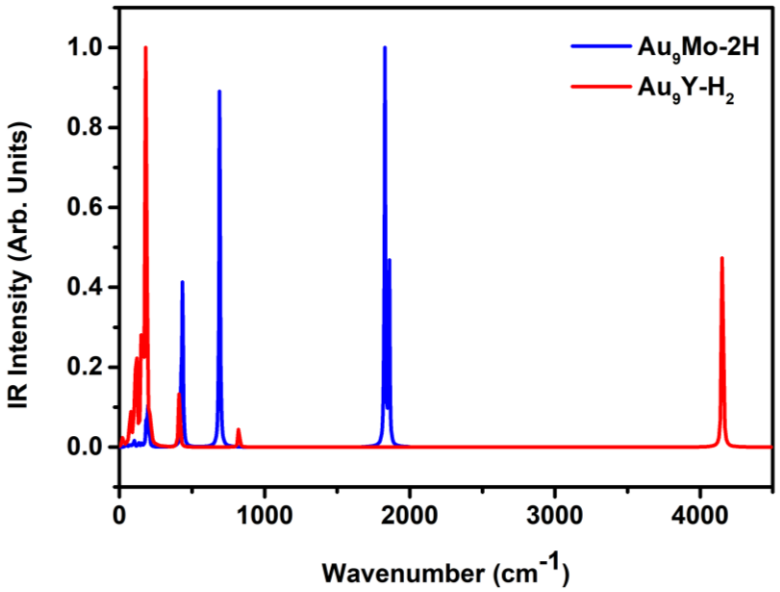

Fig. 3. IR spectra for Au_9Y-H_2 and Au_9Mo-2H clusters. The blue, and red line represent the IR spectrum of Au_9Y-H_2 and Au_9Mo-2H clusters, respectively.

For the Au_9Mo-2H cluster, the IR spectrum exhibits three peaks, representative of two main types of vibration. The peaks at 690 cm^{-1} and 1858 cm^{-1} are assigned to the asymmetric stretching mode of metal-hydrogen in the Au_9Mo framework. Conversely, the symmetric stretching mode of metal-hydrogen in the Au_9Mo host cluster is found at 1828 cm^{-1}. Finally, a bending vibration of the two hydrogen atoms is found at a wavenumber of 435 cm^{-1}. Notably, the IR spectrum of Au_9Y-H_2 shows significant differences. The spectrum features peaks at the

longer and shorter wavenumbers of 4138 cm^{-1} and 412 cm^{-1}, respectively, characteristic of symmetric stretching vibration. Two additional peaks observed at wavenumbers of 183 cm^{-1} and 819 cm^{-1} correspond to the asymmetric stretching of H-H in the Au_9Y host. The bending vibrational mode is detected at a wavenumber of 420 cm^{-1}. The results regarding the IR spectral vibrations in both molecular and dissociative adsorption serve as important initial fingerprints, providing valuable insights for future experimental studies.

4. Conclusions

In this work, we systematically compared the effects of electronic configuration on the magnetic properties and hydrogen vibrational modes of the Au_9M (M = Y and Mo) system using DFT calculations. The distorted seven-sided surface Au_9Y and cross-section of an icosahedral cage Au_9Mo have been found to be nonmagnetic and to exhibit a high magnetic moment of 3 μ_B, consistent with the electronic configurations $1S^21P^61D^4$ and $1S^21P^61D^64d_{Mo}^3$, respectively. Spin density analysis has demonstrated that the magnetic moment of the cluster is primarily attributed to the localised electrons in the d orbitals of the transition metal dopant. Additionally, we present results on the possible infrared vibrational spectra of $Au_9M@H_2$ (M = Mo and Y), which have not yet been available in the literature. We hope that our findings will contribute to the theoretical understanding of $Au_9M@H_2$ clusters and assist experimental efforts to determine the structure of Au_9M species.

CRediT author statement

Lan Ngo Thi, Dang Nguyen Van, Tung Nguyen Thanh: Conceptualisation, Funding acquisition, Data curation, Validation, Drafting of manuscript, Reviewing and editing; Hien Trinh Ngoc, Huyen Nguyen Thi Thanh, Ha Le Tien, Mai Nguyen Thi: Data curation, Formal analysis, Reviewing and editing.

ACKNOWLEDGEMENTS

This research was financially supported by the National Foundation for Science and Technology Development (NAFOSTED) under the grant number 103.01-2021.109.

COMPETING INTERESTS

The authors declare that there is no conflict of interest regarding the publication of this article.

REFERENCES

[1] M. Agrachev, S. Antonello, T. Dainese, et al. (2017), "Magnetic ordering in gold nanoclusters", *ACS Omega,* **2(6)**, pp.2607-2617, DOI: 10.1021/acsomega.7b00472.

[2] J. Botana, M. Pereiro, D. Baldomir, et al. (2008), "Magnetic-dependent structure in eight-atom gold clusters", *J. Appl. Phys.,* **103(7)**, DOI: 10.1063/1.2831336.

[3] N. Mehla, A. Mukhopadhyaya, S. Ali, et al. (2024), "Orchestration of ferro-and anti-ferromagnetic ordering in gold nanoclusters", *Nanoscale,* **16(28)**, pp.13445-13456, DOI: 10.1039/D4NR00856A.

[4] Z. Fang, X. Kuang (2014), "Hydrogen molecule adsorption on Au_nPt (n=1-12) clusters in comparison with corresponding pure Au_{n+1} (n=1-12) clusters", *Phys. Status Solidi (b),* **251(2)**, pp.446-454, DOI: 10.1002/pssb.201350170.

[5] M. Haruta, N. Yamada, T. Kobayashi, et al. (1989), "Gold catalysts prepared by coprecipitation for low-temperature oxidation of hydrogen and of carbon monoxide", *J. Catal.,* **115(2)**, pp.301-309, DOI: 10.1016/0021-9517(89)90034-1.

[6] M.W. Chang, L. Zhang, M. Davids, et al. (2020), "Dynamics of gold clusters on ceria during CO oxidation", *J. Catal.,* **392**, pp.39-47, DOI: 10.1016/j.jcat.2020.09.027.

[7] M. Haruta (1997), "Size-and support-dependency in the catalysis of gold", *Catal. Today,* **36(1)**, pp.153-166, DOI: 10.1016/S0920-5861(96)00208-8.

[8] H.W. Ghebriel, A. Kshirsagar (2007), "Adsorption of molecular hydrogen and hydrogen sulfide on Au clusters", *J. Chem. Phys.,* **126(24)**, DOI: 10.1063/1.2743420.

[9] N.T. Mai, N.T. Lan, N.T. Cuong, et al. (2021), "Systematic Investigation of the structure, stability, and spin magnetic moment of CrM_n clusters (M=Cu, Ag, Au, and n=2-20) by DFT calculations", *ACS Omega,* **6(31)**, pp.20341-20350, DOI: 10.1021/acsomega.1c02282.

[10] J. Sui, X. Wang, P. An (2014), "Geometric evolution, stability trend and electronic properties of rhenium-doped gold clusters", *Comput. Theor. Chem.,* **1028**, pp.98-105, DOI: 10.1016/j.comptc.2013.10.028.

[11] W.H. Blades, A.C. Reber, S.N. Khanna, et al. (2017), "Evolution of the spin magnetic moments and atomic valence of vanadium in VCu_x^+, VAg_x^+, and VAu_x^+ clusters (x=3-14)", *J. Phys. Chem. A,* **121(15)**, pp.2990-2999, DOI: 10.1021/acs.jpca.7b01030.

[12] C. Ehlert, I.P. Hamilton (2019), "Iron doped gold cluster nanomagnets: *ab initio* determination of barriers for demagnetization", *Nanoscale Adv.,* **1(4)**, pp.1553-1559, DOI: 10.1039/C8NA00359A.

[13] N.T. Lan, N.T. Mai, D.D. La, et al. (2022a), "DFT investigation of Au_9M^{2+} nanoclusters (M= Sc-Ni): The magnetic superatomic behavior of Au_9Cr^{2+}", *Chem. Phys. Lett.,* **793**, DOI: 10.1016/j.cplett.2022.139451.

[14] N.M. Tam, N.T. Cuong, H.T. Pham (2017), "$Au_{19}M$ (M=Cr, Mn, and Fe) as magnetic copies of the golden pyramid", *Sci. Rep.,* **7(1)**, DOI: 10.1038/s41598-017-16412-3.

[15] N.T. Lan, N.T. Mai, D.D. La, et al. (2023), "Exploring hydrogen adsorption on nanocluster systems: Insights from DFT calculations of Au_9M^{2+} (M= Sc-Ni)", *Chem. Phys. Lett.,* **831**, DOI: 10.1016/j.cplett.2023.140838.

[16] N. Rekik, M.J. Wójcik (2010), "On the influence of electrical anharmonicity on infrared bandshape of hydrogen bond", *Chem. Phys.,* **369(2-3)**, pp.71-81, DOI: 10.1016/j.chemphys.2010.02.018.

[17] N. Rekik (2017), "Signature of congregated effects of mechanical and electrical anharmonicities, Fermi resonances, and dampings on the IR spectra of hydrogen bonded systems: Quantum dynamic study", *J. Phys. Chem. A,* **121(18)**, pp.3555-3566, DOI: 10.1021/acs.jpca.7b01616.

[18] N. Rekik, S. Salman, U. Farooq, et al. (2019) "Towards accurate infrared spectral density of weak H-bonds in absence of relaxation mechanisms", *Spectrochim. Acta A Mol. Biomol. Spectrosc.,* **207**, pp.197-208, DOI: 10.1016/j.saa.2018.09.003.

[19] N. Rekik, H.T. Flakus, B. Hachula, et al. (2020a) "How far the vibrational exciton interactions are responsible for the generation of the infrared spectra of oxindole crystals?," *Spectrochim. Acta A Mol. Biomol. Spectrosc.,* **237**, DOI: 10.1016/j.saa.2020.118302.

[20] N. Rekik, N.A. Alsaif, H.T. Flakus, et al. (2020b) "A unified quantum model susceptible to elucidate the dissimilarity of IR spectral density of dicarboxylic acid crystals: Phthalic and terephthalic acid crystals cases", *Spectrochim. Acta A Mol. Biomol. Spectrosc.,* **242**, DOI: 10.1016/j.saa.2020.118728.

[21] N.V. Dang, N.T. Lan, N.T. Mai, et al. (2025a), "Hydrogen adsorption and dissociation on Au_nY (n=1-12) nanoclusters: A DFT investigation", *RSC advances,* **15(30),** pp.24668-24678, DOI: 10.1039/D5RA01901J.

[22] N.V. Dang, N.T. Lan, N. T. Mai, et al. (2025b), "DFT investigation of Au_nMo (n=2-12) Clusters: The barrierless hydrogen adsorption behavior of Au_9Mo", *Phys. Chem. Phys. Chem.,* 12pp.

[23] M. Frisch, G.W. Trucks, H.B. Schlegel, et al. (2009) "Gaussian 09, Revision a. 02, 200, gaussian", *Inc., Wallingford, CT*.

[24] P. Hohenberg, W. Kohn (1964), "Inhomogeneous electron gas", *Phys. Rev.,* **136(3B)**, DOI: 10.1103/PhysRev.136.B864.

[25] Q. Du, X. Wu, P. Wang, et al. (2020), "Structure evolution of transition metal-doped gold clusters M@ Au_{12} (M=3d-5d): Across the periodic table", *J. Phys. Chem. C,* **124(13)**, pp.7449-7457, DOI: 10.1021/acs.jpcc.9b11588.

[26] S. Neukermans, E. Janssens, H. Tanaka, et al. (2003) "Element-and size-dependent electron delocalization<? format?> in Au_NX^+ clusters (X=S c, Ti, V, Cr, Mn, Fe, Co, Ni)", *Phys. Rev. Lett.,* **90(3)**, DOI: 10.1103/PhysRevLett.90.033401.

[27] E. Janssens, H. Tanaka, S. Neukermans, et al. (2004) "Electron delocalization in Au_NX_M (X= Sc, Ti, Cr, Fe) clusters: A density functional theory and photofragmentation study", *Phys. Rev. B,* **69(8)**, DOI: 10.1103/PhysRevB.69.085402.

[28] S.S. Lu, H. Duan, Q. Li, et al. (2024) "Effects of transition metals (V, Cr, Mn, Fe and Ni) doping on magnetic properties of Co-based amorphous alloys", *J. Mater. Res. Echnol.,* **33**, pp.193-203, DOI: 10.1016/j.jmrt.2024.09.067.

[29] A. Bergman, E. Holmström, A. Niklasson, et al. (2004), "Magnetism of Fe clusters embedded in a Co matrix from first-principles theory", *Phys. Rev. B-Condensed Matter and Materials Physics,* **70(17)**, DOI: 10.1103/PhysRevB.70.174446.

[30] S. Sarugaku, M. Arakawa, T. Kawano, et al. (2019), "Electronic and geometric effects on chemical reactivity of 3*d*-transition-metal-doped silver cluster cations toward oxygen molecules", *J. Phys. Chem. C,* **123(42)**, pp.25890-25897, DOI: 10.1021/acs.jpcc.9b05117.

[31] K. Minamikawa, S. Sarugaku, M. Arakawa, et al. (2022) "Electron counting in cationic and anionic silver clusters doped with a 3d transition-metal atom: Endo-vs. exohedral geometry", *Phys. Chem. Chem. Phys.,* **24(3)**, pp.1447-1455, DOI: 10.1039/D1CP04197E.

[32] T. Höltzl, N. Veldeman, J. De Haeck (2009), "Growth mechanism and chemical bonding in scandium-doped copper clusters: Experimental and Theoretical study in Concert", *Chem. Eur. J.,* **15(16)**, pp.3970-3982, DOI: 10.1002/chem.200802372.

[33] M.A.S. Alothoum, A. Alshehab, N.A. Alsaif, et al. (2025) "IR Spectral density of υS (N-H$\vec{}$) band of 3-phenylpyrazole polymorphs: Elucidation of the synergistic influences of vibrational mode dynamics, anharmonic coupling, and direct relaxation within the framework of linear response theory", *Spectrochim. Acta A Mol. Biomol. Spectrosc.,* **347***,* DOI: 10.1016/j.saa.2025.127029.

[34] N. Rekik (2025a) "Theoretical elucidation of the IR spectra of 4-bromo-3, 5-dimethylpyrazole crystals and their deuterium-bonded analogues: Multi-objective analysis from a quantum modeling perspective", *Spectrochim. Acta A Mol. Biomol. Spectrosc.,* **341**, DOI: 10.1016/j.saa.2025.126328.

[35] N. Rekik (2025b) "Theoretical understanding of the ABC persistent structure in strongly H-bonded systems: Computational analysis of phosphonic and bis-(heptafluoropropyl) phosphonic acid dimers in gas phase", *Spectrochim. Acta A Mol. Biomol. Spectrosc.,* **337**, DOI:10.1016/j.saa.2025.126007.

[36] N. Rekik (2025c), "Deciphering the abnormal IR spectral density of phthalic acid dimer crystals: Unveiling the role of the dynamical effects of the Davydov coupling and the mechanisms of relaxation", *Spectrochim. Acta A Mol. Biomol. Spectrosc.,* **331**, DOI: 10.1016/j.saa.2025.125752.

[37] N. Rekik (2024a) "On the shape of the simulated infrared spectral density of strongly hydrogen-bonded systems: Mapping and identification of Hadži ABC structure in phosphonic acid dimers in gas phase", *Vib. Spectrosc.,* **134**, DOI: 10.1016/j.vibspec.2024.103730.

[38] N. Rekik (2024b), "IR absorption band of weak H-Bonded systems: Showcasing the signature of the quantum indirect damping within the framework of a new approach using non-Hermitean Hamiltonian formalism", *Spectrochim. Acta A Mol. Biomol. Spectrosc.,* **314**, DOI: 10.1016/j.saa.2024.124174.

[39] N.T. Lan, N.T. Mai, N.T. Cuong, et al. (2022b), "Density functional study of size-dependent hydrogen adsorption on Ag_nCr (n = 1–12) clusters", *ACS omega,* **7(42)**, pp.37379-37387, DOI: 10.1021/acsomega.2c04107.

[40] T.T. Phung, N.T. Huyen, N.T. Giang, et al. (2024), "Unraveling hydrogen adsorption on transition metal-doped $[Mo_3S_{13}]^{2-}$ clusters: Insights from density functional theory calculations", *ACS Omega,* **9(18)**, pp.20467-20476, DOI: 10.1021/acsomega.4c01557.

[41] M. Jia, J. Vanbuel, P. Ferrarim, et al. (2020), "Hydrogen adsorption and dissociation on Al_nRh^{2+} (n=1 to 9) clusters: Steric and coordination effects", *J. Phys. Chem. C,* **124(14)**, pp.7624-7633, DOI: 10.1021/acs.jpcc.9b11230.

[42] N. Rekik, A. Velcescu, P. Blaise, et al. (2001), "Spectral density of H-bonds. II. Intrinsic anharmonicity of the fast mode within the strong anharmonic coupling theory", *Chem. Phys.,* **273(1)**, pp.11-37, DOI: 10.1016/S0301-0104(01)00470-0.

[43] N. Rekik, B. Ouari, P. Blaise, et al. (2004), "IR spectral density of weak H-bonds involving quantum direct and indirect dampings. Beyond the adiabatic and harmonic approximations", *J. Mol. Struct.,* **687(1-3)**, pp.125-133, DOI: 10.1016/j.molstruc.2003.09.017.

[44] N. Rekik, F.A. Al-Agel, H.T. Flakus (2016), "Davydov coupling as a factor influencing the H-bond IR signature: Computational study of the IR spectra of 3-thiopheneacrylic acid crystal", *Chem. Phys. Lett.,* **647**, pp.107-113, DOI: 10.1016/j.cplett.2016.01.042.

[45] N. Rekik, H.T. Flakus, A.J. Jędryka, et al. (2015), "Elucidating the Davydov-coupling mechanism in hydrogen bond dimers: Experimental and theoretical investigation of the polarized IR spectra of 3-thiopheneacetic and 3-thiopheneacrylic acid crystals", *J. Phys. Chem. Solids,* **77**, pp.68-84, DOI: 10.1016/j.jpcs.2014.10.008.

[46] N. Rekik, H. Ghalla, G. Hanna (2012), "Explaining the structure of the OH stretching band in the IR spectra of strongly hydrogen-bonded dimers of phosphinic acid and their deuterated analogs in the gas phase: A computational study", *J. Phys. Chem. A,* **116(18)**, pp.4495-4509, DOI: 10.1021/jp3016084.